Optogenetic control of epileptiform activity

Jan Tønnesen[a], Andreas T. Sørensen[a], Karl Deisseroth[b], Cecilia Lundberg[c], and Merab Kokaia[a,1]

[a]Experimental Epilepsy Group, Division of Neurology, Wallenberg Neuroscience Center, Lund University Hospital, 221 00 Lund, Sweden; [b]Department of Bioengineering, Stanford University, Stanford, CA 94305; and [c]CNS Gene Therapy Unit, Department of Experimental Medical Science, Wallenberg Neuroscience Center, Lund University, 221 00 Lund, Sweden

The optogenetic approach to gain control over neuronal excitability both in vitro and in vivo has emerged as a fascinating scientific tool to explore neuronal networks, but it also opens possibilities for developing novel treatment strategies for neurologic conditions. We have explored whether such an optogenetic approach using the light-driven halorhodopsin chloride pump from *Natronomonas pharaonis* (NpHR), modified for mammalian CNS expression to hyperpolarize central neurons, may inhibit excessive hyperexcitability and epileptiform activity. We show that a lentiviral vector containing the NpHR gene under the calcium/calmodulin-dependent protein kinase IIα promoter transduces principal cells of the hippocampus and cortex and hyperpolarizes these cells, preventing generation of action potentials and epileptiform activity during optical stimulation. This study proves a principle, that selective hyperpolarization of principal cortical neurons by NpHR is sufficient to curtail paroxysmal activity in transduced neurons and can inhibit stimulation train-induced bursting in hippocampal organotypic slice cultures, which represents a model tissue of pharmacoresistant epilepsy. This study demonstrates that the optogenetic approach may prove useful for controlling epileptiform activity and opens a future perspective to develop it into a strategy to treat epilepsy.

epilepsy | hippocampus | NpHR | paroxysmal depolarizing shift (PDS) | stimulation train-induced bursting (STIB)

When archaebacterium *Natronomonas pharaonis*, living in hyperosmotic conditions of lake Zug in the Sahara desert, is exposed to light, its inward-directed halorhodopsin chloride pump (NpHR) is ativated to create a life-saving membrane potential, which drives across the membrane protons (and other cations) used for ATP synthesis (1, 2). Genetically adapted to be expressed in mammalian brain by viral vectors and optically activated with millisecond precision, the transgene NpHR pumps chloride ions into transduced neurons, hyperpolarizing and preventing them from firing action potentials (3, 4). Such powerful optical control over excitability of neuronal populations could be an attractive tool to prevent excessive activation of neurons in pathologic conditions within specific brain regions (e.g., an epileptic seizure focus). Epilepsy is a devastating neurologic condition characterized by recurrent seizures and affects approximately 1% of the general population (5, 6). One third of these patients are refractory to currently available pharmacologic treatments, leaving very few options, including surgical dissection of the epileptic focus, as an alternative. Considering the limited success and related high direct and indirect costs of epilepsy treatment for society, alternative therapeutic approaches for epileptic conditions are highly warranted. Therefore, we tested a hypothesis that epileptiform activity can be optically controlled by selective expression of NpHR in principal cells. We used a lentiviral (LV) vector containing the NpHR gene driven by the calcium/calmodulin-dependent protein kinase IIα (CaMKIIα) promoter, which expresses the transgene selectively in the principal glutamatergic neurons of the hippocampal formation (4, 7). Previously, an LV vector has been successfully used to transduce cultured hippocampal CA1–CA3 neurons with a construct containing ubiquitous EF1α promoter driving NpHR gene expression (EF1α-NpHR). These NpHR-transduced neurons were hyperpolarized

and silenced by exposure to orange light of 573–613-nm wavelength that activated the transgene NpHR (4). Selective hyperpolarization of principal neurons in the hippocampal network could result in suppression of synchronized epileptiform activity. However, intracellular accumulation of chloride due to transgene NpHR activation may theoretically change the equilibrium potential for chloride, shifting GABA$_A$ receptor–mediated hyperpolarization toward depolarization, which would result in promoting epileptiform activity. We therefore also investigated whether NpHR activation influenced GABA$_A$ receptor–mediated inhibition of the transduced cells. As an epilepsy model, we chose cultured organotypic hippocampal slices, which closely resemble pharmacoresistant epileptic tissue in humans and animal models. These slices are characterized by cell death, axonal sprouting, and synaptic reorganization, leading to increased overall excitability of the pathologic circuitry, thus having a relatively high predictive value for outcomes of future in vivo treatment (8, 9).

Results

NpHR Transgene Expression in the Hippocampal Formation. NpHR expression was assessed by including enhanced yellow fluorescent protein (EYFP) in the LV-NpHR-EYFP-pCaMKIIα vector construct (Fig. 1). Injection of 2×0.6 μL of this LV vector in vivo into postnatal day (P) 4 mice pups resulted in widespread expression of NpHR throughout the hippocampal formation, as assessed in the organotypic cultures at 21–28 days after plating the hippocampal sections from P6–8 mice pups. An example of such transgene expression in various regions of hippocampal organotypic cultures is presented in Fig. 1*A*, including dentate gyrus (DG; Fig. 1*B*), CA1 (Fig. 1*C*), and CA3 (Fig. 1*D*). Pyramidal cells in CA1 and CA3, as well as granule cells in the DG, were selectively expressing the transgene, confirming the specificity of CaMKIIα promoter for these glutamatergic principal cells. The achieved expression pattern of NpHR supported our aim to selectively target principal excitatory cells in the hippocampal formation by light illumination. Moreover, EYFP labeling of the NpHR-transduced neurons allowed for visualization of these cells in live slices to prospectively identify them for whole-cell and perforated whole-cell patch-clamp recordings. The patch pipette solutions contained biocytin, which diffused into the cells during recordings, permitting consequent confirmation of EYFP and biocytin double-labeling, to ensure that the recorded cells were transduced by transgene NpHR (Fig. 1*E*).

Intrinsic Membrane Properties of NpHR-Transduced Neurons. First we analyzed whether transduction of the neurons with NpHR could influence their membrane properties without exposure to light. In these and all other experiments, electric lights in the room
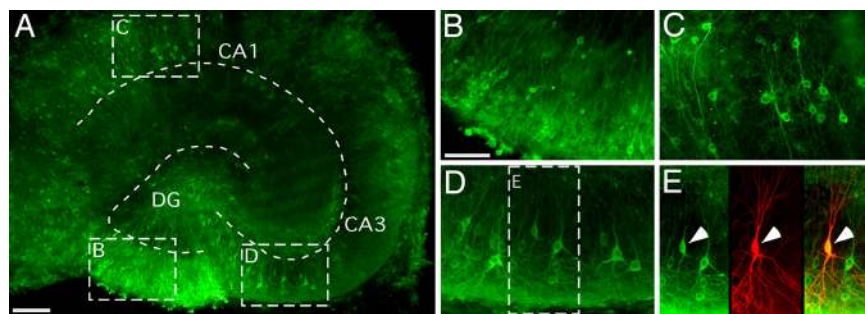

Fig. 1. NpHR expression in organotypic hippocampal slice cultures. (*A*) Epifluorescence microscopy image showing EYFP immunoreactivity in several hippocampal regions after LV-NpHR-EYFP-pCaMKIIα vector–mediated transduction. (Scale bar, 200 μm.) Boxed areas are shown magnified on the right. EYFP-labeled granule cells (*B*) in the DG, and EYFP-labeled pyramidal neurons in the CA1 (*C*) and CA3 (*D*) region of the hippocampus. (*E*) Retrospective identification of biocytin-labeled pyramidal cell in CA3 after whole-cell patch-clamp recording. Yellow indicates merged double-labeling of EYFP (FITC; green) and biocytin (Cy3; red). (Scale bar in *B*, 100 μm for *B*–*E*.)

were switched off, and the Faraday cage surrounding the recording chamber was covered with black plastic film to avoid exposure of the slices to daylight. In these experimental conditions, we compared EYFP-labeled and EYFP-negative (control) CA1 and CA3 pyramidal cells, assessing various parameters of their intrinsic and membrane properties. The results are presented in Fig. 2 *A*–*D*, supporting information (SI) Fig. S1 *A*–*C*, and Table S1. This analysis revealed no significant alterations in input resistance, resting membrane potential, action potential threshold, duration, or amplitude, as assessed by depolarizing/hyperpolarizing pulses, as well as rheobase and threshold as assessed by depolarizing ramp current application (Table S1). Accommodation of action potentials induced by a strong depolarizing current step was also similar in transduced and control CA1 and CA3 pyramidal cells, respectively (Fig. S1 *B* and *C*). In CA3 pyramidal cells, however, the current–voltage (I-V) curves were shifted toward less hyperpolarization in response to hyperpolarizing current steps (Fig. 2 *C* and *D*), which was not the case in CA1 pyramidal neurons (Fig. 2 *A* and *B*). These data suggest that expression of transgene NpHR has a relatively limited effect on general intrinsic properties and excitability of principal pyramidal cells when they are not exposed to light stimulation.

NpHR-Transduced Neurons Are Hyperpolarized by Orange Light. Next we explored whether exposure of transduced neurons to orange
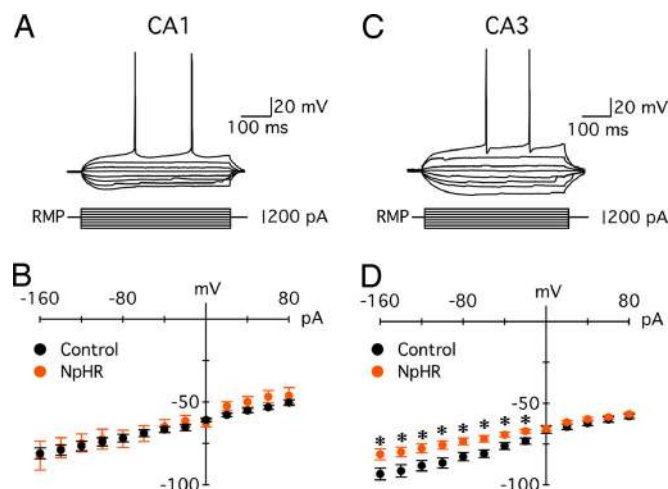
light (wavelength range, 573–613 nm) activated transgene NpHR and hyperpolarized these cells, as predicted by previous experiments (3, 4). Indeed, optical stimulation of NpHR-transduced neurons in both CA1 and CA3 areas of organotypic hippocampal cultures hyperpolarized these cells (Fig. 3 *A* and *C*, respectively). The hyperpolarization peaked initially to 18.8 ± 4.4 mV in CA1 (*n* = 10 cells) and 15.4 ± 4.3 mV for CA3 neurons (*n* = 8 cells; *P* > 0.05), gradually falling to a steady-state hyperpolarization of average 5.0 ± 1.8 mV and 4.6 ± 1.8 mV, respectively (*P* > 0.05). These observations are in good agreement with previously published data for primary dissociated CA1–CA3 hippocampal cell cultures (4). We also confirmed that the orange-light-induced hyperpolarization of NpHR-transduced pyramidal cells in CA1 and CA3 regions of organotypic cultures was effectively suppressing action potentials generated in response to injection of depolarizing currents in these cells, as shown in Fig. 3 *B* and *D*. Similar results were also obtained from NpHR-transduced pyramidal neurons in the piriform cortex (Fig. S2 *A*–*C*), suggesting that these effects were not unique for hippocampal pyramidal neurons. Taken together, these data demonstrated that optical activation of transgene NpHR induced effective hyperpolarization and silencing of action potentials in pyramidal neurons in both hippocampus and piriform cortex, areas often implicated in the generation of epileptic seizure activity [see Bertram (10)].

Hyperpolarizations were often accompanied by rebound depolarizations and action potentials at the end of the light stimulation. At resting membrane potential, these hyperpolarizations did not elicit rebound action potentials in both CA1 and
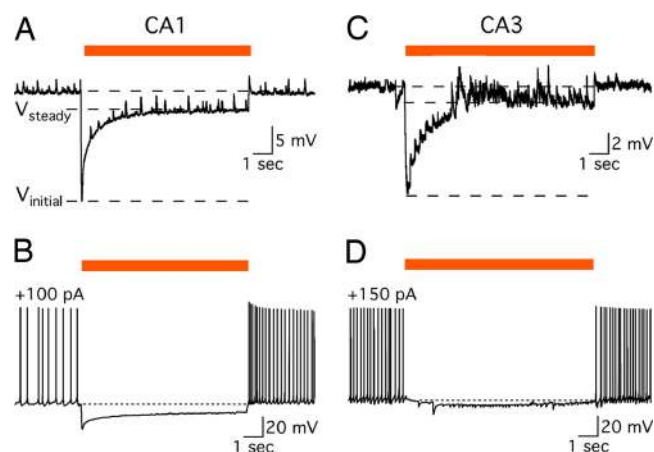

Fig. 2. I-V relationship in NpHR-transduced CA1 and CA3 pyramidal neurons. (*A* and *C*) Voltage responses in NpHR-transduced CA1 (*A*) and CA3 (*C*) pyramidal neurons during current step injections of 500-msec duration. (*B*) Averaged I-V relationship of NpHR-transduced (*n* = 12 cells) and nontransduced (*n* = 11 cells) CA1 pyramidal neurons during all steps of current injection. Note that no light is applied during these experiments. (*D*) Averaged I-V relationship curves in NpHR-transduced (*n* = 9 cells) as compared with nontransduced (*n* = 10 cells) CA3 pyramidal neurons during current step injections. Note significant differences at hyperpolarizing steps. *P < 0.05.

Fig. 3. Orange-light illumination hyperpolarizes NpHR-transduced pyramidal cells and suppresses the generation of action potentials. (*A* and *C*) Initial and steady voltage hyperpolarizations by NpHR activation in CA1 (*A*) and CA3 pyramidal (*C*) neurons. (*B* and *D*) Inhibition of current injection-induced action potentials by orange-light illumination in CA1 (*B*) and CA3 (*D*) pyramidal neurons. Bars illustrate time of light illumination.
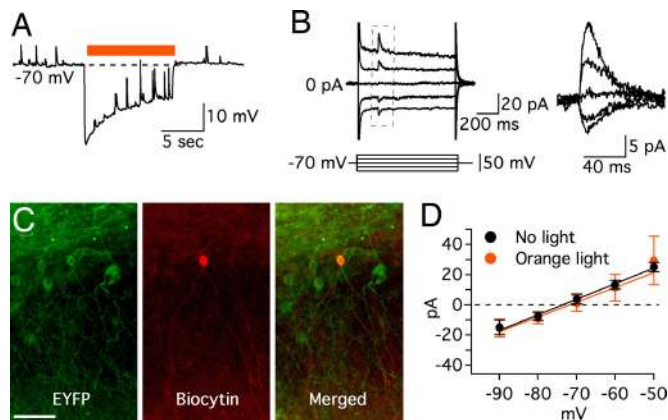
Fig. 4. The reversal potential of GABA$_A$ receptor–mediated IPSCs is unchanged by sustained orange-light activation of transgene NpHR. (*A*) Orange-light illumination hyperpolarizes NpHR-transduced EYFP-expressing granule cells recorded using perforated whole-cell patch-clamp configuration. (*B*) Voltage-clamp of the same cell as in *A* during application of 10-mV voltage steps (from −50 to −90 mV) combined with stimulation of afferent fibers generating monosynaptic IPSCs (indicated in dashed box and magnified on the right). The stimulation protocol was repeated during orange-light illumination of the organotypic slice culture. (*C*) After perforated whole-cell patch-clamp recording, the cell membrane was ruptured by negative pressure, allowing biocytin to diffuse into the cell from the attached pipette, and the recorded cell in *A* was retrospectively stained for EYFP and biocytin double-labeling (superimposed as yellow). (Scale bar, = 50 μm; applies to all images.) (*D*) Average amplitudes of evoked IPSCs plotted against the corresponding voltage step during no light and orange-light illumination (*n* = 5 cells).

CA3 pyramidal neurons (Fig. 3 *A* and *C*). However, during sustained depolarization by current injection close to threshold levels, the frequency of spontaneous action potentials increased immediately after the light-induced hyperpolarizations (Fig. 3*B*). Additional experiments revealed that both light-induced hyperpolarization of NpHR-transduced (Fig. S3*A*), as well as current-induced hyperpolarizations of NpHR-transduced and control cells (Fig. S3 *B* and *C*), elicited a brief rebound-derived increase in action potential frequencies. This increase, however, was of similar magnitude in NpHR-transduced and nontransduced CA1 and CA3 pyramidal cells, respectively (Fig. S3*D*). In concert, these data indicate that transgene NpHR does not affect generation of rebound depolarizations and action potentials.

GABA$_A$ Signaling Is Not Depolarizing in Transgene NpHR-Transduced Neurons. It has been shown previously that increased intracellular chloride concentration due to altered expression of chloride pumps at early developmental stages (11, 12), and also as a result of epileptogenesis (13, 14), transforms GABA$_A$ receptor–mediated postsynaptic potentials into depolarizations. Because NpHR chloride pump activation generates chloride ion flow into the transduced cells, we asked whether accumulation of chloride intracellularly might lead to GABA$_A$ receptor–mediated inhibitory postsynaptic potentials (IPSPs) becoming depolarizing, thus potentially increasing activation of neurons and promoting epileptiform activity. To address this question, we used perforated whole-cell patch-clamp recordings to avoid alteration of intracellular chloride concentration by the pipette solution. For this particular experiment, we chose NpHR-transduced dentate granule cells for their relatively small cell soma size to be able to achieve better control over the membrane potential during perforated whole-cell patch-clamp recordings. All recorded cells were confirmed to express transgene NpHR by hyperpolarization in response to orange light (Fig. 4*A*). Monosynaptic inhibitory postsynaptic currents (IPSCs) in NpHR-transduced dentate granule cells were induced by stimulating their inhibitory

afferent fibers while the cell membrane potential was incrementally stepped from −50 mV to −90 mV to reveal GABA-mediated IPSC reversal potential in conditions where the slices were exposed to orange light (continuously pumping chloride intracellularly). Comparison of the same parameters was made from the same cells without light exposure (Fig. 4*B*). The stimulation-induced IPSCs showed fast kinetics typical of perisomatic inhibitory synapses (fast rise and fall time and relatively short duration of 50–60 ms; Fig. 4*B*). The average reversal potential for IPSCs was estimated to be −73.2 mV (95% confidence interval, −85.5 to −62.4 mV) during orange-light exposure, and was not different from that when they were not exposed to light (−73.8 mV; 95% confidence interval, −79.5 to −68.6 mV; Fig. 4*D*). All recorded cells were confirmed to be labeled for EYFP and biocytin (Fig. 4*C*). These data show that activation of transgene NpHR does not alter the reversal potential for the GABA$_A$ receptor–mediated IPSCs and therefore does not transform IPSPs into depolarizations. Thus, we found no evidence that transgene NpHR activation promotes excitability or epileptiform activity by converting GABA$_A$ receptor–mediated hyperpolarizations into depolarizations in the current in vitro epilepsy model.

Optical Activation of Transgene NpHR Suppresses Epileptiform Activity In Vitro. The results of the previous section encouraged us to explore whether hyperpolarization and silencing of the pyramidal cells by optical activation of transgene NpHR would also be sufficient to inhibit pathologic epileptiform activity [stimulation train-induced bursting (STIB)] in the hippocampal organotypic cultures. First, we confirmed that transgene NpHR per se, without light stimulations, does not promote epileptiform activity. The threshold for STIB induction, duration of STIB, and frequencies of spikes during STIB were not different between nonilluminated NpHR-transduced and nontreated slices (Table S2). Next, in NpHR-transduced slices, we induced STIB during orange-light (573–613 nm) illumination. As a control, slices were not exposed to any light, or they were exposed to spectrally separated blue light (420–480 nm), which normally does not activate NpHR (4). As shown in Figs. 5 and 6, exposure of NpHR-transduced slices to orange light substantially shortened the duration of STIB discharges both in CA3 (Fig. 5*A*) and CA1 (Fig. 6*A*) regions of the hippocampus (depicted as relative changes in Fig. 5*B* and Fig. 6*B*). Exposure of the same slices to blue light had no effect on STIB duration in the CA1 region (Fig. 6 *A* and *B*). Average data derived from these experiments show a significant decrease in STIB duration during orange-light exposure as compared with control (no light) or blue-light exposure both in CA3 [STIB1 (control): 12.2 ± 3.1 sec; STIB2 (orange): 6.4 ± 3.5 sec; STIB3 (control): 9.6 ± 2.9 sec; *n* = 7 slices] and CA1 [STIB1 (control): 22.1 ± 3.9 sec; STIB2 (orange): 3.7 ± 1.7 sec; STIB3 (blue): 16.2 ± 2.5 sec; *n* = 9 slices] regions of the hippocampus. To exclude that the observed effect on STIB was due to a possible refractoriness of the slices to generate STIB at a given interstimulus interval, an additional control experiment was performed by inducing 3 consecutive STIBs at the same interstimulus interval but without any light exposure. This showed a stable STIB induction by all 3 consecutive stimulations both in CA3 (Fig. 5*B*, control, *n* = 5 slices) and CA1 (Fig. 6*B*, control, *n* = 5 slices) regions. These data show that optical activation of transgene NpHR can effectively suppress epileptiform activity in a relevant model of pharmacoresistant epilepsy in vitro.

Optical Activation of Transgene NpHR Suppresses Epileptiform Bursting Activity in CA3 Pyramidal Neurons. To further substantiate our findings with field recordings and to address the mechanisms by which transgene NpHR activation suppresses epileptiform activity, we proceeded to assess the effect of transgene NpHR on
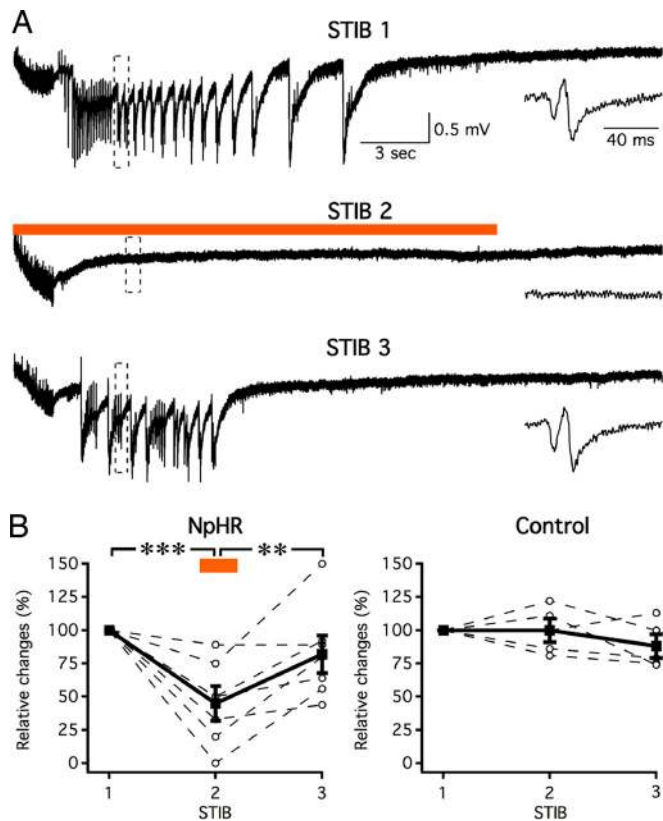
Fig. 5. STIB in CA3 is strongly attenuated by orange-light activation of transgene NpHR in organotypic hippocampal cultures. (*A*) Recordings of 3 consecutive STIB stimulations, with orange-light illumination on second stimulation, in NpHR-transduced slices. *Insets*: Magnification of traces showing epileptiform bursts after STIB stimulation. Scale bars apply for all traces. (*B*) Relative changes in STIB duration of individual recordings (dotted lines and open circles) and their average values (mean $\pm$ SEM; solid line and squares) for NpHR and nontransduced control slices, respectively, during 3 consecutive STIB. **$P < 0.01$; ***$P < 0.001$.

Fig. 6. STIB in CA1 is strongly attenuated by orange-light activation of transgene NpHR in organotypic hippocampal cultures. (*A*) Recordings of 3 consecutive STIB stimulations, with orange-light illumination on second stimulation, in NpHR-transduced slices. *Insets*: Magnification of traces showing spikes during STIB. Scale bars apply for all traces. (*B*) Relative changes in STIB duration of individual recordings (dotted lines and open circles) and their average values (mean $\pm$ SEM; solid line and filled squares) for NpHR and nontransduced control slices, respectively, during 3 consecutive STIB. At STIB2, orange light is applied to NpHR-transduced slices as indicated by orange bar. At STIB3, blue light is applied to NpHR-transduced slices as indicated by blue bar. ***$P < 0.001$.

epileptiform burst discharges in individual CA3 pyramidal neurons during STIB by whole-cell patch-clamp recordings (Fig. 7). The STIB was reflected in CA3 pyramidal neurons as a series of paroxysmal depolarizing shifts (PDS) with superimposed action potentials, the occurrence of which lasted on average for 35.3 ± 15.1 sec and 29.1 ± 11.8 sec for control STIB1 and STIB3, respectively (Fig. 7). Exposure of slices to orange light during intermediate STIB2 significantly shortened the duration of PDS occurrence in NpHR-transduced CA3 pyramidal cells to 7.9 ± 3.7 sec ($n = 8$ cells) while leaving the average number of action potentials per PDS unaltered [STIB1: 3.0 ± 1.1; STIB2 (orange light): 2.2 ± 0.7; STIB3: 2.3 ± 0.5; $n = 6$ NpHR-transduced cells; STIB1: 2.3 ± 0.5; STIB2: 2.2 ± 0.4; STIB3: 2.1 ± 0.3; $n = 9$ control cells; $P > 0.05$], as illustrated in Fig. 7 *A* and *B*. Averaged relative changes are demonstrated in Fig. 7*C*, whereby the total duration of PDS occurrence decreased by approximately 75% in transduced CA3 pyramidal neurons but was unaffected in control cells ($n = 9$ cells). Inhibition of PDS occurrence was possible to induce repeatedly by orange-light illumination ($n = 3$ cells; Fig. 7*D*). The PDS generated by repeated STIB in NpHR-transduced CA3 pyramidal neurons were unaltered when slices were not exposed to orange light (Fig. 7*D*). In addition to STIB, during whole-cell patch-clamp recordings in CA3, we used another in vitro model for epileptiform activity induced by bath application of picrotoxin (a GABA$_A$ receptor antagonist usually inducing epileptiform activity in in-vitro brain slices). Also in this
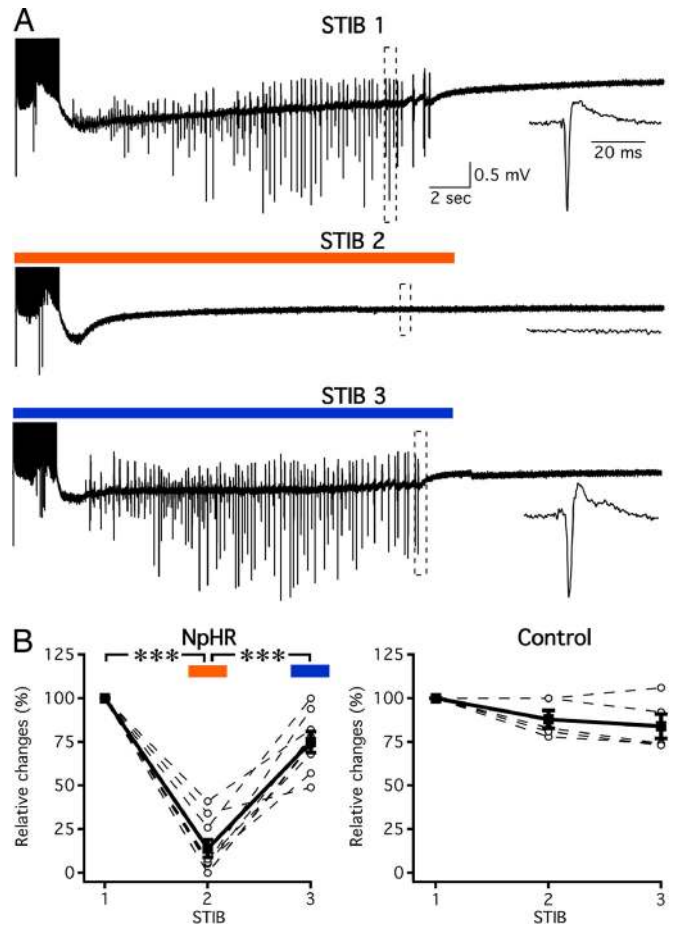
model, we observed that generation of high-frequency action potential trains induced by picrotoxin could be strongly inhibited by optical activation of transgene NpHR in CA1 pyramidal neurons, as exemplified in Fig. S4 *A* and *B*.

Taken together, these data demonstrate that the duration of PDS occurrence was effectively suppressed in NpHR-transduced CA3 pyramidal neurons and could explain suppression of epileptiform activity (STIB) in the CA3 area. Similar inhibition of PDS most likely also occurs in pyramidal neurons of CA1 and piriform cortex.

Discussion

Here, using field and whole-cell patch-clamp recordings, we show that optogenetic treatment with an LV vector containing the NpHR gene can suppress epileptiform activity in the epileptic hippocampus. We also show that the inhibitory effect of optical stimulation on epileptiform activity (STIB) is mediated by hyperpolarization and suppression of PDS generation in principal hippocampal neurons, which are selectively targeted by the CaMKIIα promoter driving NpHR expression.
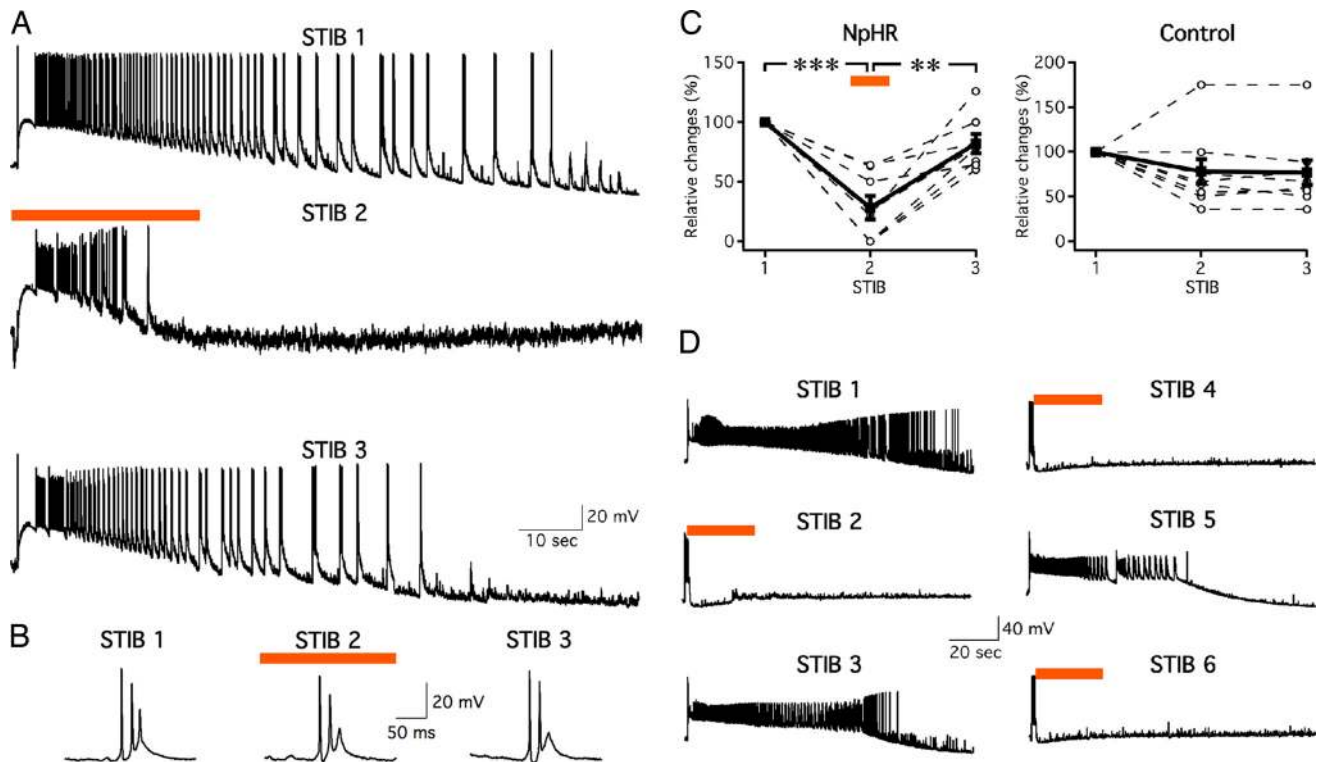
Fig. 7. PDS occurrence during STIB in NpHR-transduced CA3 pyramidal neurons during STIB is strongly inhibited by orange-light stimulation. (*A*) PDS in CA3 pyramidal cell recorded by whole-cell patch-clamp during 3 consecutive STIB. (*B*) Light activation of NpHR (shown by orange bar) at STIB2 reduces the duration of PDS occurrence without changing number of action potentials per PDS. (*C*) Relative changes in duration of PDS occurrence recorded in individual neurons (indicated by dotted lines and open circles) and average values, indicated by solid line (mean ± SEM), for NpHR-transduced and nontransduced CA3 pyramidal neurons. (*D*) Repeated orange-light illumination (intermediated by control stimulations without light exposure) repeatedly inhibits STIB-generated PDS occurrence by activation of NpHR. **$P < 0.01$; ***$P < 0.001$.

Our data suggest that expression of transgene NpHR per se does not lead to any major alterations in membrane or other intrinsic properties of the transduced neurons, although some aggregation of EYFP has been reported in transgenic animals expressing NpHR under EF1α promoter (15, 16). In this study, we exclusively recorded from those cells that had no visible signs of such EYFP fragmentation. Nevertheless, we detected a shift of I-V curves selectively in CA3 neurons toward more inward rectification during hyperpolarizing current steps. One of the explanations could be increased expression of Kir channels (17) in these neurons. It is not clear, though, how NpHR could have induced such increased expression of Kir channels, and moreover, in a cell-specific manner exclusively in CA3 pyramidal neurons (given that no such changes in I-V curves were observed in CA1 pyramidal neurons). This possible change in inward rectification may reduce hyperpolarizations of CA3 cells induced by transgene NpHR light activation, although epileptiform activity was still reliably blocked in these slices.

Activation of transgene NpHR had no effect on IPSCs induced by afferent inhibitory synapses on the transduced neurons, even with prolonged exposures to the orange light. This finding is of major importance, particularly considering the possibility of using an optogenetic approach with NpHR for epilepsy treatment. These results may seem counterintuitive, because accumulation of chloride ions intracellularly should lead to a shift in the chloride equilibrium potential toward depolarization, converting IPSPs into depolarizing potentials, which may generate action potentials (14). Thus, inhibitory GABAergic inputs may become "excitatory," and instead of inhibiting the principal cells could have induced their activation. However, the amount of chloride ions transported across the cell membrane by activated

transgene NpHR seems to be in the range that the endogenous chloride pumps [e.g., the KCC2 that normally pumps chloride ions out of neurons (18)] are able to effectively normalize. Therefore, possible NpHR-induced changes in chloride reversal potential, transforming IPSPs into depolarizations, do not occur under the present conditions.

Regulating neuronal excitability with optogenetic manipulations is a powerful, although relatively unexplored, approach for functional studies of neuronal circuits. Using this approach, it is possible to selectively activate or inhibit certain neuronal populations in distinct regions and thus reveal specific contributions of neuronal populations in integrative function of the brain. Some fundamental questions of neuroscience have already been addressed by application of optogenetic approaches, particularly using channelrhodopsin-2 (19, 20), e.g., for identification of functional efferent synaptic outputs from adult newborn dentate granule cells (21), activating specific motor cortical behavior (22), defining the role of hypocretin neurons in sleep–wakefulness arousal systems located in the posterior hypothalamus (23) in mice, or dissecting mechanisms of deep brain stimulation in Parkinsonian rodents (24). Our own data identify the role of NpHR-mediated silencing of excitatory principal cells in suppressing epileptiform activity in mouse hippocampal organotypic cultures. We show that selective hyperpolarization of a limited population of principal hippocampal neurons by optical stimulation is sufficient to significantly inhibit focal epileptiform activity. We also show that without light stimulation, transgene NpHR expression does not per se alter the excitability of transduced neurons and does not promote epileptiform activity in the neuronal networks of transduced hippocampal slices. Our findings have important implications, not only for expanding our

knowledge on mechanisms of seizure generation; they may also raise some practical considerations of controlling epileptiform activity in the hippocampus, which is one of the major regions in temporal lobe epilepsy, where intractable seizures often originate (see ref. 10). In fact, organotypic hippocampal cultures are considered a reliable model for testing different treatment approaches for suppressing pharmacoresistant epilepsy (8). The idea of controlling excitability of neurons in patients to correct activity just in specific target neurons, while leaving other neurons unaltered, is an appealing but challenging prospect, particularly when designing safe and biocompatible light-delivery devices. This is a necessary step toward translation of such technology into clinical use. Our study provides a proof of principle, although in vitro, that such devices could be used in the future for patients with temporal lobe epilepsy. One could speculate that implantable optogenetic devices can be coupled to implantable seizure onset–predicting devices (25) that would trigger optical stimulation in a timely manner to prevent forthcoming epileptic episodes. Despite such a fascinating perspective, many questions remain to be addressed. Although epileptiform activity in organotypic cultures is an ideal model for pharmacoresistant epilepsy, it still needs to be shown that such an optogenetic approach could be applied in in-vivo epilepsy models to suppress seizures. The present study is an encouraging step in establishing a foundation for future development in this direction.

Materials and Methods

Animals. BALB/c mice were housed under a 12/12-h light cycle with ad libitum access to water and food. All experimental procedures were approved by the Lund Ethical Committee for Experimental Animals (M8506).

Organotypic Cultures and Viral Vector Administration. Organotypic hippocampal cultures were prepared from LV-NpHR–injected P6–8 BALB/c brains and cultured as previously described (26–28). The LV-NpHR-EYFP-pCaMKIIα vector (4) was produced as previously described (29) and injected into hippocampus or piriform cortex at P4, before dissection and preparation for organotypic cultures (see *SI Methods*).

Electrophysiology. Recordings were made in hippocampal slices cultured for 3 weeks (30). Intrinsic membrane properties of whole-cell recorded neurons, as well as rheobase and action potential accommodation at strong depolarizations, were determined as previously (ref. 30; *SI Methods*). Rebound action potentials after light illumination (rebound) were compared with rebound action potentials induced by current injections (*SI Methods*).

IPSCs were recorded from dentate gyrus granule cells as described previously (31). Amplitudes of induced IPSCs were obtained at membrane potentials from −50 mV to −90 mV at 10-mV increments. The reversal potential, with and without orange-light illumination, was determined by plotting the amplitude of IPSCs against corresponding membrane potentials (*SI Methods*).

Field recordings were obtained through a glass capillary filled with artificial CSF, having a tip resistance of 1 to 2 MΩ. STIB was induced by a train of 1-msec square pulses of 7–25 V at 60 Hz for 2 sec delivered via a bipolar stainless steel stimulating electrode, as described previously (31). Threshold of STIB corresponded to the voltage at which a single 1-msec pulse stimulation would elicit a population spike in field recordings or an action potential in whole-cell recordings. STIB was defined as 2 or more consecutive field discharge (field recordings) or PDS (whole-cell recordings) events with amplitudes of at least 2 times the amplitude of mean signal noise following immediately after the stimulation, and individual discharges not being temporally separated by more than 2 sec (*SI Methods*). In whole-cell recordings, action potentials per PDS were analyzed during the initial 4 sec after STIB (*SI Methods*). The interstimulation interval for STIB induction was 5 min. Orange light was applied at the onset of the 2-sec stimulation and continued for 20 sec. All data acquisition was performed as previously described (30). Orange and blue light was applied using specific excitation filters on a mercury lamp, as previously (ref. 4; *SI Methods*).

Immunohistochemistry. Immunohistochemistry was performed as previously described, using Ab290 (Abcam) to recognize EYFP (ref. 30; *SI Methods*).

Statistics. Differences in duration of STIB (field recordings) and PDS occurrence (whole-cell patch-clamp recordings) were analyzed using a paired *t* test. A paired *t* test was also used to compare amplitudes of evoked IPSCs at different membrane potentials during perforated whole-cell patch-clamp recordings. ANOVA followed by a Bonferroni-Dunn post hoc test was used for rebound depolarization and rebound action potential analysis, whereas an unpaired Student's *t* test was used to compare all other parameters between groups. The level of significance was set at $P < 0.05$. All data are presented as mean ± SEM.

1. Falb M, et al. (2005) Living with two extremes: Conclusions from the genome sequence of *Natronomonas pharaonis*. *Genome Res* 15:1336–1343.
2. Kolbe M, Besir H, Essen LO, Oesterhelt D (2000) Structure of the light-driven chloride pump halorhodopsin at 1.8 A resolution. *Science* 288:1390–1396.
3. Zhang F, Aravanis AM, Adamantidis A, de Lecea L, Deisseroth K (2007) Circuit-breakers: Optical technologies for probing neural signals and systems. *Nat Rev Neurosci* 8:577–581.
4. Zhang F, et al. (2007) Multimodal fast optical interrogation of neural circuitry. *Nature* 446:633–639.
5. Banerjee PN, Hauser WA (2008) Incidence and prevalence. *Epilepsy: a comprehensive textbook*, eds Engel JJ, Pedley T (Wolters Kluwer/Lippincott Williams & Wilkins, Baltimore), 2nd Ed, pp 45–56.
6. Hauser WA, Annegers JF, Kurland LT (1991) Prevalence of epilepsy in Rochester, Minnesota: 1940–1980. *Epilepsia* 32:429–445.
7. Dittgen T, et al. (2004) Lentivirus-based genetic manipulations of cortical neurons and their optical and electrophysiological monitoring in vivo. *Proc Natl Acad Sci USA* 101:18206–18211.
8. Albus K, Wahab A, Heinemann U (2008) Standard antiepileptic drugs fail to block epileptiform activity in rat organotypic hippocampal slice cultures. *Br J Pharmacol* 154:709–724.
9. Bausch SB, McNamara JO (2000) Synaptic connections from multiple subfields contribute to granule cell hyperexcitability in hippocampal slice cultures. *J Neurophysiol* 84:2918–2932.
10. Bertram EH (2009) Temporal lobe epilepsy: Where do the seizures really begin? *Epilepsy Behav* 14(Suppl 1):32–37.
11. Cherubini E, Rovira C, Gaiarsa JL, Corradetti R, Ben Ari Y (1990) GABA mediated excitation in immature rat CA3 hippocampal neurons. *Int J Dev Neurosci* 8:481–490.
12. Leinekugel X, et al. (1999) GABA is the principal fast-acting excitatory transmitter in the neonatal brain. *Adv Neurol* 79:189–201.
13. Rivera C, Voipio J, Kaila K (2005) Two developmental switches in GABAergic signalling: The K+-Cl- cotransporter KCC2 and carbonic anhydrase CAVII. *J Physiol* 562(Pt 1):27–36.
14. Staley KJ (2008) Does plasticity of the GABA(A) reversal potential contribute to epileptogenesis? *Epilepsy Curr* 8:107–110.
15. Gradinaru V, Thompson KR, Deisseroth K (2008) eNpHR: A *Natronomonas* halorhodopsin enhanced for optogenetic applications. *Brain Cell Biol* 36:129–139.
16. Zhao S, et al. (2008) Improved expression of halorhodopsin for light-induced silencing of neuronal activity. *Brain Cell Biol* 36:141–154.
17. Isomoto S, Kondo C, Kurachi Y (1997) Inwardly rectifying potassium channels: Their molecular heterogeneity and function. *Jpn J Physiol* 47:11–39.
18. Payne JA (1997) Functional characterization of the neuronal-specific K-Cl cotransporter: Implications for [K+]o regulation. *Am J Physiol* 273(5 Pt 1):C1516–C1525.
19. Boyden ES, Zhang F, Bamberg E, Nagel G, Deisseroth K (2005) Millisecond-timescale, genetically targeted optical control of neural activity. *Nat Neurosci* 8:1263–1268.
20. Zhang F, Wang LP, Boyden ES, Deisseroth K (2006) Channelrhodopsin-2 and optical control of excitable cells. *Nat Methods* 3:785–792.
21. Toni N, et al. (2008) Neurons born in the adult dentate gyrus form functional synapses with target cells. *Nat Neurosci* 11:901–907.
22. Aravanis AM, et al. (2007) An optical neural interface: In vivo control of rodent motor cortex with integrated fiberoptic and optogenetic technology. *J Neural Eng* 4:S143–S156.
23. Adamantidis AR, Zhang F, Aravanis AM, Deisseroth K, de Lecea L (2007) Neural substrates of awakening probed with optogenetic control of hypocretin neurons. *Nature* 450:420–424.
24. Gradinaru V, Mogri M, Thompson KR, Henderson JM, Deisseroth K (2009) Optical deconstruction of parkinsonian neural circuitry. *Science* 324:354–359.
25. Aziz JN, et al. (2006) Towards real-time in-implant epileptic seizure prediction. *Conf Proc IEEE Eng Med Biol Soc* 1:5476–5479.
26. Rytter A, Cronberg T, Asztely F, Nemali S, Wieloch T (2003) Mouse hippocampal organotypic tissue cultures exposed to in vitro ''ischemia'' show selective and delayed CA1 damage that is aggravated by glucose. *J Cereb Blood Flow Metab* 23:23–33.
27. Stoppini L, Buchs PA, Muller D (1991) A simple method for organotypic cultures of nervous tissue. *J Neurosci Methods* 37:173–182.
28. Benninger F, et al. (2003) Functional integration of embryonic stem cell-derived neurons in hippocampal slice cultures. *J Neurosci* 23:7075–7083.
29. Jakobsson J, Ericson C, Jansson M, Bjork E, Lundberg C (2003) Targeted transgene expression in rat brain using lentiviral vectors. *J Neurosci Res* 73:876–885.
30. Jakubs K, et al. (2006) Environment matters: Synaptic properties of neurons born in the epileptic adult brain develop to reduce excitability. *Neuron* 52:1047–1059.
31. Stasheff SF, Bragdon AC, Wilson WA (1985) Induction of epileptiform activity in hippocampal slices by trains of electrical stimuli. *Brain Res* 344:296–302.

NEUROSCIENCE